

# Efficient organic-inorganic hybrid Schottky solar cell: The role of built-in potential

Yawen Zhu, Tao Song, Fute Zhang, Shuit-Tong Lee, and Baoquan Sun<sup>a)</sup>

Jiangsu Key Laboratory for Carbon-Based Functional Materials & Devices, Institute of Functional Nano & Soft Materials (FUNSOM), Soochow University, 199 Ren'ai Road, Suzhou 215123, China

(Received 6 February 2013; accepted 5 March 2013; published online 19 March 2013)

The organic-inorganic hybrid Schottky solar cells based on solution processed poly(3,4-ethylenedioxythiophene):poly(styrenesulfonate) (PEDOT:PSS) in combination with silicon offer the merits of simple fabrication process and potential low cost. Here, we demonstrate that the work function (WF) of PEDOT:PSS films plays a critical role on the electronic output characteristics of the device. The WF of PEDOT:PSS is tuned by adding an aqueous solution of perfluorinated ionomer (PFI) due to its high electron affinity, which is compatible to fabricate the hybrid Si/PEDOT:PSS device. With an addition of 4% (weight) PFI into PEDOT:PSS, the device achieves a fill factor (FF) as high as 0.70 without sacrifice of open-circuit voltage and short-circuit current density, which improves 20% in comparison with the pristine PEDOT:PSS (0.58). The detailed electrical output measurements reveal that the high FF is ascribed to the enhanced built-in potential as well as suppression of charge recombination at organic-inorganic interface. © 2013 American Institute of Physics. [<http://dx.doi.org/10.1063/1.4796112>]

Schottky solar cells based on metal/semiconductor junctions are intensively investigated due to their simple structures and high light to electricity power conversion efficiency (PCE), and great efforts have been made to improve their performance.<sup>1–3</sup> Tuning metal work function (WF) is an efficient method to provide built-in potential across the interface, which is favorable to sweeping charge into the proper directions.<sup>4</sup> Unfortunately, the performance of the Si/metal Schottky solar cells is relatively insensitive to the metal WF because of the formation of metal silicides during vacuum metal deposition on silicon.<sup>5</sup> Therefore, in order to avoid silicide formation, carbon nanotubes (CNTs) as well as graphene as conducting layer have been utilized to form Schottky junction with silicon. Rapid progresses have been made and PCE of up to ~8% for graphene and ~15% for CNTs have been achieved.<sup>6,7</sup>

Recently, poly(3,4-ethylenedioxythiophene):poly(styrenesulfonate) (PEDOT:PSS), as solution processed high conducting conjugated polymer,<sup>8</sup> has been widely incorporated with the silicon to fabricate the organic-inorganic hybrid devices.<sup>9,10</sup> The hybrid devices provide the merit of solution-process fabrication with simple device structure, which may potentially drop the cost of device. PEDOT:PSS acts as transporting electrode to replace metal, and n-type silicon (n-Si) conducts light harvesting layer to generate charge. It has been reported that the WF of PEDOT:PSS can be tuned from ~5.0 eV to ~5.7 eV by controlling the chemical composition of the film surface,<sup>11</sup> electrochemical doping,<sup>12</sup> layer-by-layer ionic self-assembly, and post-deposition treatment.<sup>13</sup> Unfortunately, all these methods are incompatible with the PEDOT:PSS/Si hybrid solar cell.

In this report, perfluorinated ionomer (PFI) was employed to tune the WF of PEDOT:PSS in order to explore the effect on the Schottky solar cells. The WF of PEDOT:PSS played a

critical role on the electric output characteristics of the hybrid devices. With addition of 4% (weight) PFI, the device yielded a fill factor (FF) of 0.70, which improved 20% compared with the pristine PEDOT:PSS (0.58). The transient electric output characteristics have been used to explore the device performance with various WF of PEDOT:PSS.

The device structure of the Schottky solar cells was depicted in Figure 1(a). Clean n-Si substrates were treated by a two-step chlorination/alkylation process according to a previously reported method.<sup>14,15</sup> Highly conductive PEDOT:PSS (CLEVIOS PH 1000) (1 wt. % in water) was mixed with various volumes of PFI (0.5 wt% in water and isopropanol), resulting in series of solution containing PFI to PEDOT:PSS ratio of 0.4%, 2%, 4%, and 6% (w/w, PFI/PEDOT:PSS). The chemical structures of PEDOT:PSS and PFI were showed in Figure 1(b). PEDOT:PSS solutions doped with different concentrations of PFI were spin coated onto Si substrates and then annealed in glovebox at 125 °C for 30 min. Silver grid electrodes were deposited onto organic layer for efficient hole collection. Finally, back Ohmic contacts were obtained by depositing In:Ga eutectic metal. The edges of the device were covered with stainless steel mask and the area for illumination was 0.8 cm<sup>2</sup>.

In order to explore the WF of PEDOT:PSS layer effect on the organic/Si hybrid Schottky solar cell, various amounts of PFI were added to tune WF of PEDOT:PSS. The WF of PEDOT:PSS were estimated by means of the scanning Kelvin probe microscope (SKPM) method. The relation between WF of the conductive tip,  $\Phi_t$ , and the samples,  $\Phi_s$ , is given by

$$\Phi_s = \Phi_t - eV_{\text{CPD}}, \quad (1)$$

where  $e$  is the elementary charge and  $V_{\text{CPD}}$  is the surface potential measured by SKPM.<sup>16,17</sup> As shown in Figures 2(a)–2(c), the surface potential of PFI was about 400 mV more negative than that of PEDOT:PSS layer. This potential

<sup>a)</sup>Email: bqsun@suda.edu.cn. Tel.: (86)-512-65880820. Fax: (86)-512-65882846.

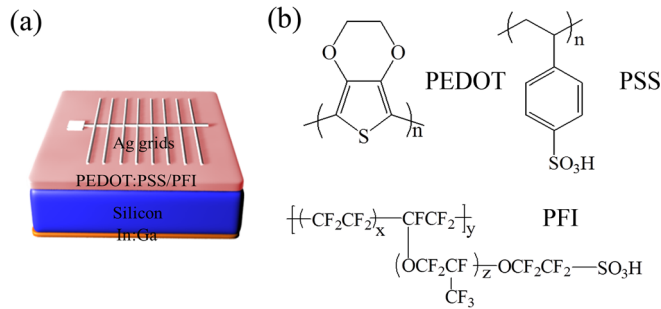


FIG. 1. (a) Schematic of Schottky solar cell based on n-Si and PEDOT:PSS with various concentrations of PFI. (b) Chemical structures of PEDOT:PSS and PFI.

difference was caused by the lower ionization potential level and higher dipole moment of PFI, which led to formation of strong dipole between PEDOT:PSS and PFI.<sup>18,19</sup> In Figure 2(d), as the concentration of PFI increased from undoped to 4%, the surface potential of the composite films decreased about 170 mV, which revealed that WF level increased about 0.17 eV ( $\Delta\Phi \approx 0.17$  eV). When the concentration of PFI reached 6%, the WF value was enlarged to 0.3 eV higher than that of unmodified PEDOT:PSS film. The measured corresponding surface potential images of different films were showed in Figure S1(a–e) (see Ref. 20).

Figure 3(a) displayed the current density-voltage (J-V) characteristics of Schottky solar cells based on planar n-Si and PEDOT:PSS with and without 4% PFI under AM 1.5 and light intensity of 100 mA/cm<sup>2</sup>. The parameters for the devices with various concentrations of PFI were summarized in Table I. It was observed that as the concentration of PFI increased from undoped to 4%, the value of PCE improved obviously from 8.2% to 9.9%, and the FF of the hybrid solar

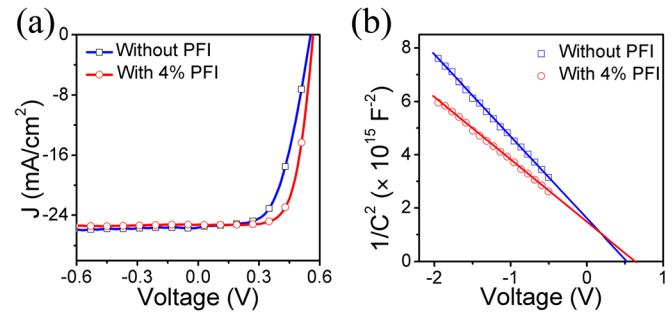


FIG. 3. (a) Electric Output characteristics of Schottky solar cells based on n-Si and PEDOT:PSS with and without 4% PFI under AM 1.5 and light intensity of 100 mA/cm<sup>2</sup>. (b) 1/C<sup>2</sup>-V plots of corresponding Schottky solar cells.

cell followed the same trend as the PFI content growing. However, the device performance began to drop at the higher concentration of PFI (6%).

It was well known that the film morphology also played a critical role on the device performance. The optical microscopy images of PEDOT:PSS films with different concentrations of PFI were illustrated as Figure S2 in Ref. 20. From Figure S2(a)–(e), it was found that as the concentration of PFI increased from undoped to 4%, the film surface showed tiny change. However, obvious defect regions appeared on the film surface with increased concentration (6%) of PFI, which would deteriorate of device performance. This phenomenon may be ascribed to the striation formation during spin coating process because of the poor solubility of PFI.<sup>21</sup> Although the WF of PEDOT:PSS film with 6% PFI increased obviously, the device performance tended to be poor due to the unfavorable film morphology. The sheet resistance and the conductivity value were also measured and summarized in Table SI (see Ref. 20). It was found that the conductivity of the films exhibited neglectable difference when modified with PFI from 203 Ω/□ (unmodified PEDOT:PSS) to 183 Ω/□ (4% PFI added into PEDOT:PSS). Therefore, the FF was not the matter of conductivity of PEDOT:PSS film.

To further explore the effect of increased WF of PEDOT:PSS on the device performance, the capacitance versus bias voltage (C-V) characteristics were also obtained as Figure 3(b), which were used to analyze the built-in potential ( $V_{bi}$ ) for the Schottky junction. According to the Schottky Mott relation,

$$1/C^2 = 2(V + V_{bi})/eN_D\epsilon_s\epsilon_0, \quad (2)$$

in which V is the bias voltage,  $N_D$  is the doping level of the semiconductor, and  $\epsilon_s$ ,  $\epsilon_0$  are permittivity of vacuum and

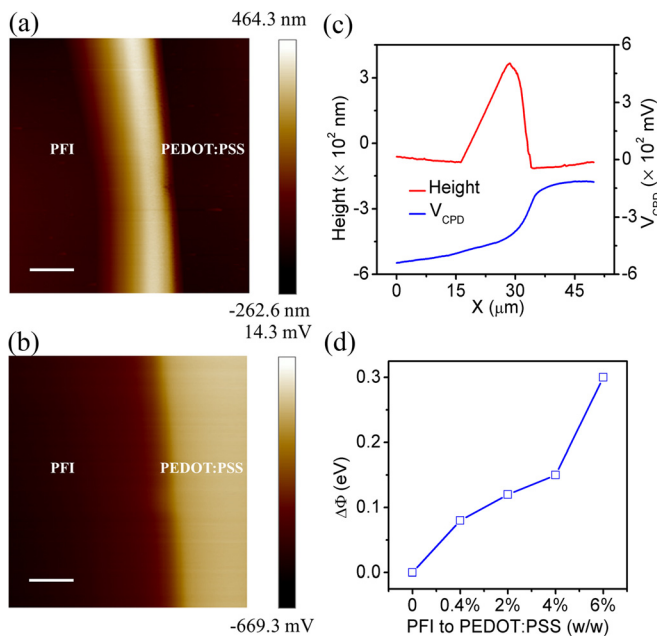


FIG. 2. (a) Topographic image and (b) surface potential image of PEDOT:PSS (right part) and PFI (left part). Both the scale bars are 10 μm. (c) Cross-sectional line profile of the topographic and surface potential ( $V_{CPD}$ ) images. (d) WF difference of PEDOT:PSS films modified with various concentrations of PFI ( $\Delta\Phi$ ), and WF of PEDOT:PSS without PFI was used as reference.

TABLE I. Summary of electric output characteristics of Schottky solar cells based on n-Si and PEDOT:PSS with various concentrations of PFI.

Concentration of PFI (%)	$V_{oc}$ (V)	$J_{sc}$ (mA/cm <sup>2</sup> )	FF	PCE (%)	Series resistance (Ω·cm <sup>2</sup> )
Undoped	0.55	25.58	0.58	8.20	6.00
0.4	0.55	25.26	0.61	8.45	5.69
2	0.55	26.22	0.65	9.32	3.85
4	0.56	25.26	0.70	9.90	3.29
6	0.55	25.81	0.64	9.02	3.97

semiconductor, respectively. In this model, the  $1/C^2$  scaled linearly with  $V$  and the extrapolation to the abscissa yields  $V_{bi}$ .<sup>6,22</sup> It was observed that  $V_{bi}$  increased by 0.07 V from 0.56 V to 0.63 V after doping with 4% PFI. The larger  $V_{bi}$  would bring in a wider depletion region, thus leading to better separation of photo generated carries and decreased the direct bulk recombination. Therefore, the higher FF of the 4% PFI doped devices was attributed to the larger  $V_{bi}$ .

The transient photovoltaic measurements (TPVs) were carried out according to previous reports.<sup>23–25</sup> A 532 nm diode laser was used as the optical perturbation. The pulse duration was set to be 1  $\mu$ s and the repetition rate to be 100 Hz. To change the  $V_{oc}$  from 0.1 V to 0.57 V, the photovoltage transients were measured over an equivalent intensity range of 0.001–1 sun. The peak value of the voltage transient was fixed to be 10 mV and the current transient was measured at an impedance of 50  $\Omega$ . The voltage and photocurrent transient results of hybrid Schottky cells made from PEDOT:PSS with and without 4% concentration of PFI were plotted as Figure S3 in Ref. 20. The carrier lifetime of those devices were obtained by fitting the voltage transient curve according to the equation

$$\delta V = \Delta V_0 \exp(-t/T), \quad (3)$$

in which  $\Delta V_0$  is the peak value of voltage transient (10 mV),  $t$  is the decay time, and  $T$  is the carrier lifetime. The fitting results were illustrated as Figure S4 in Ref. 20. The capacitance at each  $V_{oc}$  was calculated by

$$\Delta \Phi = \int_0^t I dt, \quad (4)$$

$$C = \Delta Q / \Delta V_0, \quad (5)$$

where  $I$  is the value of transient photocurrent. At last, the carrier concentration was acquired by integrating the capacitance over voltage

$$N = \frac{1}{Aed} \int_0^{V_{oc}} C dV, \quad (6)$$

where  $A$  is the device area,  $e$  is electronic charge, and  $d$  is the device thickness. The calculated curves of capacitance and carrier concentration versus  $V_{oc}$  were showed in Figure 4(a).

As shown in Figure 4(b) and summarized in Table S2 (see Ref. 20), the device with 4% PFI obtained the longer carrier lifetime and lower carrier concentration. Since the

carrier concentration corresponded to the stored charge in the bulk of the junction, which was also proportional to the trap state density. The lower carrier concentration and longer carrier life time of the device indicated enhanced charge separation and collection, thus further leading to less carrier recombination. Here, the device based on 4% PFI doped PEDOT:PSS displayed much lower carrier concentration of  $1.01 \times 10^{13} \text{ cm}^{-3}$  as well as longer carrier life time of 37.5  $\mu$ s than pristine one, which is consistent with its improved FF.

In summary, the WF of PEDOT:PSS film played a critical role on the performance of n-Si based Schottky solar cells. The WF level of PEDOT:PSS could be increased by adding a perfluorinated polymer of PFI due to its high electron affinity. By adding 4% PFI into PEDOT:PSS, the device achieved a FF of 0.70, which improved 20% compared to the non-treated one. Through the steady and transient electrical output characterizing, it was verified that the high FF was ascribed to the enhanced built-in potential as well as suppression of charge recombination at organic-inorganic interface. Such organic/inorganic Schottky solar cells can potentially further deliver high performance combined with better film morphology and higher WF.

This work was supported by the National Basic Research Program of China (973 Program) (2012CB932402), National Natural Science Foundation of China (91123005, 60976050, 61176057, 61211130358), the Natural Science Foundation of Jiangsu Province (BK2010003), Scientific Research Foundation for the Returned Overseas Chinese Scholars of State Education Ministry.

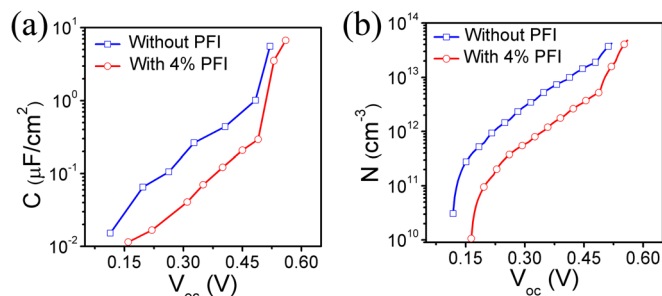


FIG. 4. (a) Differential capacitance ( $C$ ) vs.  $V_{oc}$  and (b) carrier concentration ( $N$ ) vs.  $V_{oc}$  for Schottky solar cells based on n-Si and PEDOT:PSS with and without 4% PFI.

- <sup>1</sup>X. Li, H. Zhu, K. Wang, A. Cao, J. Wei, C. Li, Y. Jia, Z. Li, X. Li, and D. Wu, *Adv. Mater.* **22**, 2743 (2010).
- <sup>2</sup>Z. Li, V. P. Kunets, V. Saini, Y. Xu, E. Dervishi, G. J. Salamo, A. R. Biris, and A. S. Biris, *ACS Nano* **3**, 1407 (2009).
- <sup>3</sup>J. M. Luther, M. Law, M. C. Beard, Q. Song, M. O. Reese, R. J. Ellingson, and A. J. Nozik, *Nano Lett.* **8**, 3488 (2008).
- <sup>4</sup>J. Robertson, *Phys. Status Solidi A* **207**, 261 (2010).
- <sup>5</sup>S. Maldonado, D. Knapp, and N. S. Lewis, *J. Am. Chem. Soc.* **130**, 3300 (2008).
- <sup>6</sup>X. Miao, S. Tongay, M. K. Petterson, K. Berke, A. G. Rinzier, B. R. Appleton, and A. F. Hebard, *Nano Lett.* **12**, 2745 (2012).
- <sup>7</sup>E. Shi, L. Zhang, Z. Li, P. Li, Y. Shang, Y. Jia, J. Wei, K. Wang, H. Zhu, D. Wu, S. Zhang, and A. Cao, *Sci. Rep.* **2**, 884 (2012).
- <sup>8</sup>J. Ouyang, Q. Xu, C.-W. Chu, Y. Yang, G. Li, and J. Shinar, *Polymer* **45**, 8443 (2004).
- <sup>9</sup>L. N. He, C. Y. Jiang, H. Wang, D. Lai, and Rusli, *Appl. Phys. Lett.* **100**, 073503 (2012).
- <sup>10</sup>X. Shen, B. Sun, D. Liu, and S.-T. Lee, *J. Am. Chem. Soc.* **133**, 19408 (2011).
- <sup>11</sup>T.-W. Lee and Y. Chung, *Adv. Funct. Mater.* **18**, 2246 (2008).
- <sup>12</sup>F. Zhang, A. Petr, H. Peisert, M. Knupfer, and L. Dunsch, *J. Phys. Chem. B* **108**, 17301 (2004).
- <sup>13</sup>J. Huang, P. F. Miller, J. S. Wilson, A. J. de Mello, J. C. de Mello, and D. D. C. Bradley, *Adv. Funct. Mater.* **15**, 290 (2005).
- <sup>14</sup>M. Y. Bashouti, T. Stelzner, S. Christiansen, and H. Haick, *J. Phys. Chem. C* **113**, 14823 (2009).
- <sup>15</sup>H. Haick, P. T. Hurley, A. I. Hochbaum, P. Yang, and N. S. Lewis, *J. Am. Chem. Soc.* **128**, 8990 (2006).
- <sup>16</sup>L. Sun, J. Wang, and E. Bonaccorso, *J. Phys. Chem. C* **114**, 7161 (2010).
- <sup>17</sup>V. Palermo, M. Palma, and P. Samorì, *Adv. Mater.* **18**, 145 (2006).
- <sup>18</sup>T. W. Lee, Y. Chung, O. Kwon, and J. J. Park, *Adv. Funct. Mater.* **17**, 390 (2007).
- <sup>19</sup>T. W. Lee, O. Kwon, M. G. Kim, S. H. Park, J. Chung, S. Y. Kim, Y. Chung, J. Y. Park, E. Han, D. H. Huh, J. J. Park, and L. Pu, *Appl. Phys. Lett.* **87**, 231106 (2005).

- <sup>20</sup>See supplementary material at <http://dx.doi.org/10.1063/1.4796112> for hybrid Schottky solar cell characterization.
- <sup>21</sup>D. P. Birnie, *J. Mater. Res.* **16**, 1145 (2001).
- <sup>22</sup>Q. Liu, M. Ono, Z. Tang, R. Ishikawa, K. Ueno, and H. Shirai, *Appl. Phys. Lett.* **100**, 183901 (2012).
- <sup>23</sup>A. H. Ip, S. M. Thon, S. Hoogland, O. Voznyy, D. Zhitomirsky, R. Debnath, L. Levina, L. R. Rollny, G. H. Carey, A. Fischer, K. W. Kemp, I. J. Kramer, Z. Ning, A. J. Labelle, K. W. Chou, A. Amassian, and E. H. Sargent, *Nat. Nanotechnol.* **7**, 577 (2012).
- <sup>24</sup>C. G. Shuttle, B. O'Regan, A. M. Ballantyne, J. Nelson, D. D. C. Bradley, J. de Mello, and J. R. Durrant, *Appl. Phys. Lett.* **92**, 093311 (2008).
- <sup>25</sup>Z. Li, F. Gao, N. C. Greenham, and C. R. McNeill, *Adv. Funct. Mater.* **21**, 1419 (2011).